

Human Brain Mapping

Copy of e-mail Notification

Human Brain Mapping Published by John Wiley & Sons, Inc.

Dear Author,

Your article page proofs for Human Brain Mapping is ready for your final content correction within our rapid production workflow. The PDF file found at the URL given below is generated to provide you with a proof of the content of your manuscript. Once you have submitted your corrections, the production office will proceed with the publication of your article.

John Wiley & Sons has made this article available to you online for faster, more efficient editing. Please follow the instructions below and you will be able to access a PDF version of your article as well as relevant accompanying paperwork.

First, make sure you have a copy of Adobe Acrobat Reader software to read these files. This is free software and is available for user downloading at (<http://www.adobe.com/products/acrobat/readstep.html>).

Open your web browser, and enter the following web address:

<http://cps.kwglobal.com/jw/retrieval.aspx>

You will be prompted to log in, and asked for a password. Your login name will be your email address, and your password will be f0009c0c465a

Example:

Login: your e-mail address

Password: f0009c0c465a

The site contains one file, containing:

Author Instructions Checklist

Annotated PDF Instructions

Reprint Order Information

Color Charge Form

A copy of your page proofs for your article

In order to speed the proofing process, we strongly encourage authors to correct proofs by annotating PDF files. Any corrections should be returned to HBMprod@wiley.com 1 to 2 business days after receipt of this email in order

Human Brain Mapping

Copy of e-mail Notification

to achieve our goal of publishing your article online 15 days from the day final data was received.

Please see the Instructions on the Annotation of PDF files included with your page proofs. Please take care to answer all queries on the last page of the PDF proof; proofread any tables and equations carefully; and check that any Greek characters (especially μ) have converted correctly. Please check your figure legends carefully.

answer all queries on the last page of the PDF proof
proofread any tables and equations carefully
check your figure(s) and legends for accuracy

Your article cannot be published until we have received your completed license agreement. If you have not already done so, please log in into Author Services (<https://authorservices.wiley.com>) and click on "My Dashboard." When you locate your article on the Dashboard, please click the button that says "Sign License" to use the Wiley Author Licensing Service (WALS) to complete your license agreement.

Within 1 to 2 business days please return page proofs with corrections and any relevant forms to:

Production Editor, HBM
Email: HBMprod@wiley.com

Technical problems? If you experience technical problems downloading your file or any other problem with the website listed above, please contact Balaji (e-mail: Wiley.CS@cenveo.com, phone: +91 (44) 4205-8810 (ext.308)). Be sure to include your article number.

Questions regarding your article? Please don't hesitate to contact me with any questions about the article itself, or if you have trouble interpreting any of the questions listed at the end of your file. REMEMBER TO INCLUDE YOUR ARTICLE NO. (23735) WITH ALL CORRESPONDENCE. This will help us address your query most efficiently.

As this e-proofing system was designed to make the publishing process easier for everyone, we welcome any and all feedback. Thanks for participating in our e-proofing system!

This e-proof is to be used only for the purpose of returning corrections to the publisher.

Sincerely,

Production Editor, HBM
Email: HBMprod@wiley.com



Additional reprint purchases

Should you wish to purchase additional copies of your article, please click on the link and follow the instructions provided:

<https://caesar.sheridan.com/reprints/redir.php?pub=10089&acro=HBM>

Corresponding authors are invited to inform their co-authors of the reprint options available.

Please note that regardless of the form in which they are acquired, reprints should not be resold, nor further disseminated in electronic form, nor deployed in part or in whole in any marketing, promotional or educational contexts without authorization from Wiley. Permissions requests should be directed to mail to: permissionsus@wiley.com

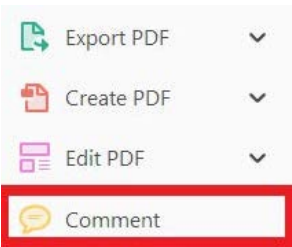
For information about 'Pay-Per-View and Article Select' click on the following link: wileyonlinelibrary.com/aboutus/ppv-articleselect.html

USING e-ANNOTATION TOOLS FOR ELECTRONIC PROOF CORRECTION


Required software to e-Annotate PDFs: Adobe Acrobat Professional or Adobe Reader (version 8.0 or above). (Note that this document uses screenshots from Adobe Reader DC.)
The latest version of Acrobat Reader can be downloaded for free at: <http://get.adobe.com/reader/>

Once you have Acrobat Reader open on your computer, click on the [Comment](#) tab (right-hand panel or under the Tools menu).


This will open up a ribbon panel at the top of the document. Using a tool will place a comment in the right-hand panel. The tools you will use for annotating your proof are shown below:

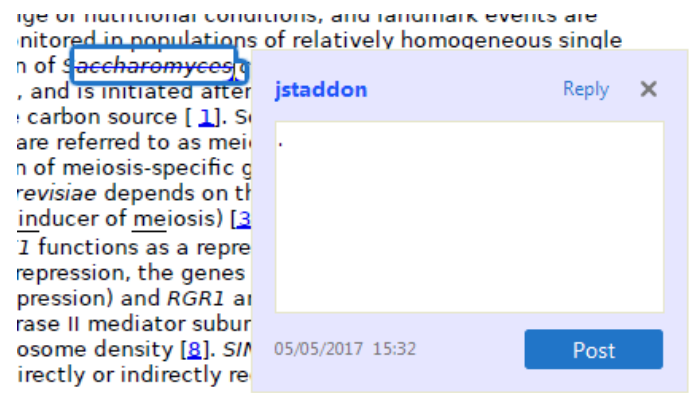


1. **Replace (Ins)** Tool – for replacing text.


 Strikes a line through text and opens up a text box where replacement text can be entered.

How to use it:


- Highlight a word or sentence.
- Click on .
- Type the replacement text into the blue box that appears.



2. **Strikethrough (Del)** Tool – for deleting text.

 Strikes a red line through text that is to be deleted.



How to use it:

- Highlight a word or sentence.
- Click on .
- The text will be struck out in red.



experimental data if available. For ORFs to be had to meet all of the following criteria:

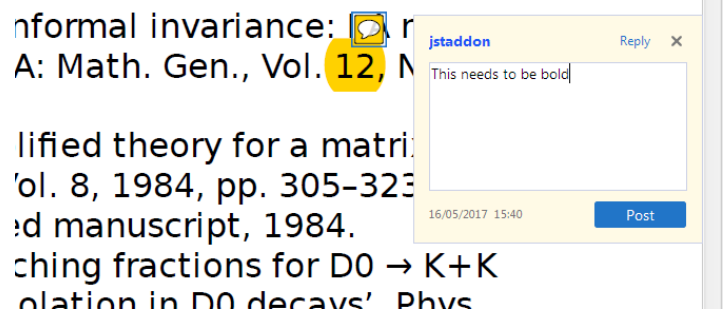
1. Small size (~~35~~-250 amino acids).
2. Absence of similarity to known proteins.
3. Absence of functional data which could not be the real overlapping gene.
4. Greater than 25% overlap at the N-terminus with another coding feature; over both ends; or ORF containing a tRNA.

3. **Commenting** Tool – for highlighting a section to be changed to bold or italic or for general comments.


  Use these 2 tools to highlight the text where a comment is then made.

How to use it:


- Click on .
- Click and drag over the text you need to highlight for the comment you will add.
- Click on .
- Click close to the text you just highlighted.
- Type any instructions regarding the text to be altered into the box that appears.

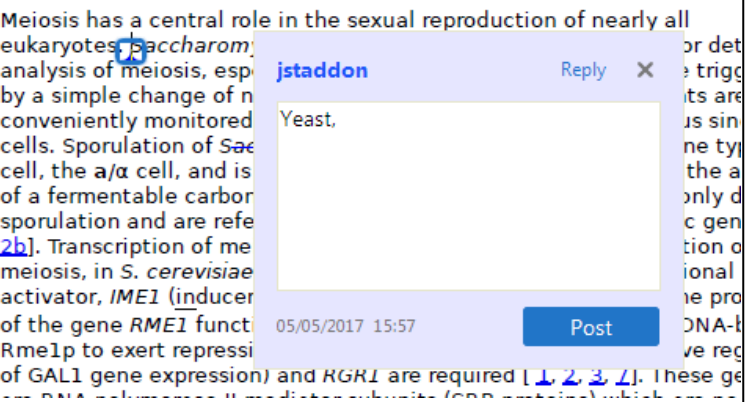


4. **Insert** Tool – for inserting missing text at specific points in the text.


 Marks an insertion point in the text and opens up a text box where comments can be entered.

How to use it:


- Click on .
- Click at the point in the proof where the comment should be inserted.
- Type the comment into the box that appears.



5. **Attach File** Tool – for inserting large amounts of text or replacement figures.

 Inserts an icon linking to the attached file in the appropriate place in the text.


How to use it:

- Click on  .
- Click on the proof to where you'd like the attached file to be linked.
- Select the file to be attached from your computer or network.
- Select the colour and type of icon that will appear in the proof. Click OK.


The attachment appears in the right-hand panel.

chondrial preparator
ative damage injury
e extent of membra
i, malondialdehyde (TBARS) formation. I
used by high perform

6. **Add stamp** Tool – for approving a proof if no corrections are required.

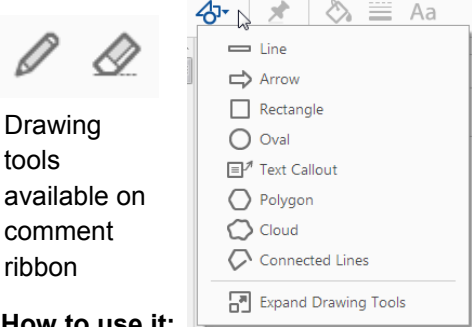
 Inserts a selected stamp onto an appropriate place in the proof.

How to use it:

- Click on  .
- Select the stamp you want to use. (The **Approved** stamp is usually available directly in the menu that appears. Others are shown under *Dynamic*, *Sign Here*, *Standard Business*).
- Fill in any details and then click on the proof where you'd like the stamp to appear. (Where a proof is to be approved as it is, this would normally be on the first page).

of the business cycle, starting with the
on perfect competition, constant ret
production. In this environment goods
extra profits and hence a transfer of market
he market for the good is not identical. It
etermined by the model. The New-Key
otaki (1987), has introduced produc
general equilibrium models with nomin
and demand shocks. Most of this literat

APPROVED

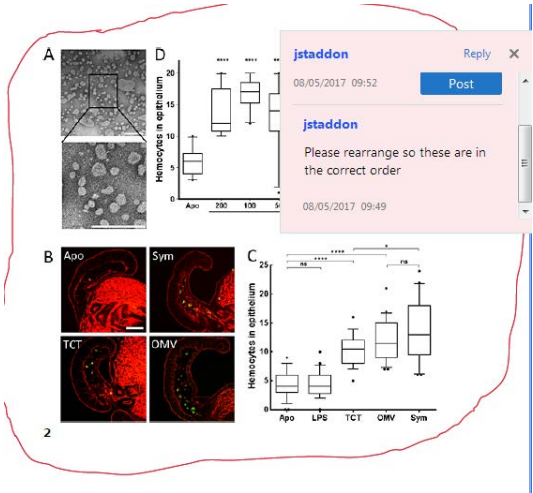


How to use it:

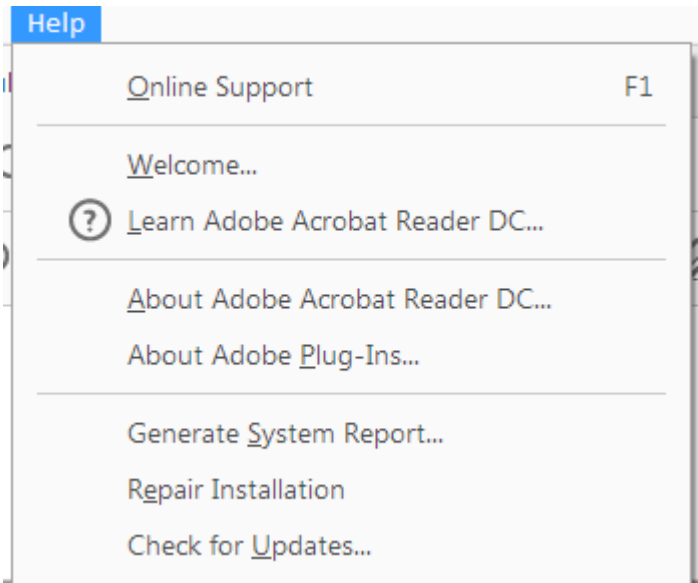
- Click on one of the shapes in the **Drawing Markups** section.
- Click on the proof at the relevant point and draw the selected shape with the cursor.
- To add a comment to the drawn shape, right-click on shape and select *Open Pop-up Note*.
- Type any text in the red box that appears.

7. **Drawing Markups** Tools – for drawing shapes, lines, and freeform annotations on proofs and commenting on these marks.

Allows shapes, lines, and freeform annotations to be drawn on proofs and for comments to be made on these marks.



For further information on how to annotate proofs, click on the **Help** menu to reveal a list of further options:



WILEY

COLOR REPRODUCTION IN YOUR ARTICLE

Color figures were included with the final manuscript files that we received for your article. Because of the high cost of color printing, we can only print figures in color if authors cover the expense. **The charge for printing figures in color is \$500 per figure.**

Please indicate if you would like your figures to be printed in color or black and white. Color images will be reproduced online in *Wiley Online Library* at no charge, whether or not you opt for color printing.

Failure to return this form will result in the publication of your figures in black and white.

JOURNAL HUMAN BRAIN MAPPING (HBM) VOLUME _____ ISSUE _____

TITLE OF MANUSCRIPT _____

MS. NO. _____ NO. OF COLOR PAGES _____ AUTHOR(S) _____

☐ Please print my figures in black and white

☐ Please print my figures in color

\$ _____

BILL TO:

Name _____

Institution _____

Address _____

Purchase

Order No. _____

Phone _____

Fax _____

E-mail _____

Neural Signature of Inattentive Deafness

AQ3

**Gautier Durantin,^{1,2,3} Frederic Dehais,² Nicolas Gonthier,^{1,2}
Cengiz Terzibas,⁴ and Daniel E. Callan^{1,2,4*}**

¹Center for Information and Neural Networks (CiNet), National Institute of Information and Communications Technology (NICT), Osaka University, Osaka, Japan

²Institut Supérieur de l'Aéronautique et de l'Espace (ISAE), Université Fédérale Toulouse Midi-Pyrénées, Toulouse, France

³School of Information Technology and Electrical Engineering, The University of Queensland, Brisbane, Australia

⁴Multisensory Cognition and Computation Laboratory, Universal Communication Research Institute, National Institute of Information and Communications Technology, Kyoto, Japan

Abstract: Inattentive deafness is the failure to hear otherwise audible sounds (usually alarms) that may occur under high workload conditions. One potential cause for its occurrence could be an attentional bottleneck that occurs when task demands are high, resulting in lack of resources for processing of additional tasks. In this fMRI experiment, we explore the brain regions active during the occurrence of inattentive deafness using a difficult perceptual-motor task in which the participants fly through a simulated Red Bull air race course and at the same time push a button on the joystick to the presence of audio alarms. Participants were instructed to focus on the difficult piloting task and to press the button on the joystick quickly when they noticed an audio alarm. The fMRI results revealed that audio misses relative to hits had significantly greater activity in the right inferior frontal gyrus IFG and the superior medial frontal cortex. Consistent with an attentional bottleneck, activity in these regions was also present for poor flying performance (contrast of gates missed versus gates passed for the flying task). A psychophysiological interaction analysis from the IFG identified reduced effective connectivity to auditory processing regions in the right superior temporal gyrus for missed audio alarms relative to audio alarms that were heard. This study identifies a neural signature of inattentive deafness in an ecologically valid situation by directly measuring differences in brain activity and effective connectivity between audio alarms that were not heard compared to those that were heard. *Hum Brain Mapp* 00:000–000, 2017. © 2017 Wiley Periodicals, Inc.

Key words: inattentive deafness; neuroergonomics; attentional bottleneck; fMRI; attention; perception; auditory; aviation; workload; connectivity

Contract grant sponsor: Center for Information and Neural Networks; Contract grant sponsor: National Institute of Information and Communications Technology; Contract grant sponsor: AXA Research Fund ("Neuroergonomics for flight safety" Chair program).

*Correspondence to: Daniel Callan; Center for Information and Neural Networks (CiNet), National Institute of Information and Communications Technology (NICT), Osaka University, 1-4

Yamadaoka, Suita City, Osaka 565-0871, Japan.

E-mail: dcallan@nict.go.jp

Received for publication 10 January 2017; Revised 10 July 2017; Accepted 11 July 2017.

DOI: 10.1002/hbm.23735

Published online 00 Month 2017 in Wiley Online Library (wileyonlinelibrary.com).

INTRODUCTION

Audio and video alarms are often used to alert one to an impending hazardous situation. The inability to detect these unexpected warning signals is a safety issue in many domains [Murphy et al., 2011; Dehais et al., 2012; Hasanain et al., 2017]. Some theories explain this phenomenon as a result of working memory limitations (a phenomenon called “inattentional amnesia”; c.f. Wolfe [1999], Kreitz et al. [2016]), or a failure in the triggering in late change-related cortical responses [Puschmann et al. 2013]. However, there is now a strong corpus of evidence that high perceptual or attentional load affects visual cortex activations to the extent that unexpected visual stimuli may remain unnoticed [Rauss et al., 2009; Lavie et al., 2014]. This phenomenon is known as inattentional blindness. However, little is known about the neural mechanisms underpinning auditory cue misperception. There is a crucial need to address this issue as a persistent lack of conscious awareness of auditory alarms has been linked to several aviation accidents [Bliss, 2003; Dehais et al., 2010]. This absence of awareness to auditory alarms has been generally explained in terms of poor design (i.e., stressing and aggressive) and lack of alarm reliability leading to immediate action cancellation on the alarm control panel (known as the “cry wolf effect” [Cvach, 2012]). More recently, research has considered the reduction of attentional resources to account for this phenomenon. Less known than its visual counterpart, the inattentional deafness hypothesis postulates that the detection of auditory cues is attenuated when engaged in a visually demanding task [Causse, 2016; Kreitz et al., 2016; Lavie et al., 2014; MacDonald & Lavie, 2011; Molloy et al., 2015]. This attenuation is exhibited especially when they are task-irrelevant [Tellinghuisen et al., 2016]. Studies in the aeronautical context [Dehais et al. 2012, 2014] confirmed that such a phenomenon could take place in the cockpit as pilots mainly rely on visual information to operate the aircraft. For instance, experiments involving high mental demand in flight simulators [Scannella et al., 2016] and in actual flight conditions [Callan et al., 2016] led to high rates of inattentional deafness with both studies showing, respectively, 56% and 55.85% missed auditory alarms.

There is still debate whether the visual and auditory resources can be divided by modality, and to some extent act independently, to perform tasks [Wickens, 1984; Keitel et al., 2013]. A body of literature provides evidence that attention is shared between modalities at a central level [Brand-D’Abrescia & Lavie, 2008; Santangelo et al., 2007; Scannella et al., 2016; Sinnett et al., 2006]. A reasonable hypothesis is that each modality has its own limited pool of resources at the perceptual level, but when these modalities compete for goals achievement, shielding against overload and resource depletion is implemented through top-down priority-based modulatory processes [Awh et al., 2006; Vachon and Tremblay, 2008]. Consistent with this theory, the lateral prefrontal cortex, inferior frontal gyrus (IFG), superior medial frontal cortex SMFC, and bilateral insula have been identified as potential sites representing a central

attentional bottleneck [Dux et al., 2006; Szameitat et al., 2016; Tombu et al., 2011]. The term “bottleneck” is here used as proposed by Craik [1948], that is, as being related to the limited processing capacity of the brain. As a consequence, the term “attentional bottleneck” described in the article refers to the active mechanism affording task processing using the limited brain capacity. In our study, the activity of this bottleneck is visible through attenuation of perceptual processes under excessive load conditions.

Some authors postulate that such gating mechanisms may also exist at a lower cortical integrative level such as the posterior middle temporal gyrus (MTG) and superior temporal sulcus (STS) [Molloy et al., 2016] via direct visual-auditory connections [see Macaluso & Driver [2005] and Calvert and Thesen [2004] for reviews]. Studies have revealed that the auditory evoked responses can be suppressed by modulatory influences at an early perceptual stage [Scannella et al. 2013] and at a later attentional stage [Giraudet et al., 2015] or both perceptual and attentional stages [Molloy et al., 2016]. This modulation is associated with lower superior temporal gyrus (STG) activations [Rinne et al., 2007; Molloy et al., 2016; Giraudet et al., 2015]. In addition, attentional load can modulate the activity of early parts of the auditory pathway such as the inferior colliculus [Rinne et al., 2008]. More surprisingly, the recording of the auditory brainstem response suggested that visual load could even modulate auditory processing before reaching the thalamus and the auditory cortex areas [Sörqvist et al., 2012].

While most of the inattentional deafness experiments have been conducted with basic laboratory tasks, very few studies have evaluated the neural signature of this phenomenon in ecological conditions, such as during real or simulated flight. Studies that aimed at characterizing inattentional deafness in ecological conditions have focused on the use of electroencephalography (EEG) [Giraudet et al., 2015; Scannella et al., 2016]. However, the low spatial resolution of this method together with its inability to assess the activation of subcortical or closed-field structures of the brain limits its use to characterize fully the mechanisms at the origin of inattentional deafness.

In this article, we present the results from the first investigation of inattentional deafness in ecological conditions using a brain-imaging device with high spatial resolution. A simulated piloting task was performed in an fMRI scanner. Control of the aircraft was implemented using a joystick. The task involved both video and audio alarms, and was a modified version of the Red Bull Air Race [Callan et al., 2012] that generated a high level of workload for participants. The choice was made to replicate demanding situations prone to elicit alarm misperceptions with a sufficient rate to perform miss versus hit contrast. This was to guarantee that we could assess the activation of brain regions specifically associated with inattentional deafness phenomenon, a scientific goal that has never been achieved before. In particular, the objective was to identify the potential role of an attentional bottleneck in the establishment of this phenomenon.

♦ Neural Signature of Inattentional Deafness ♦

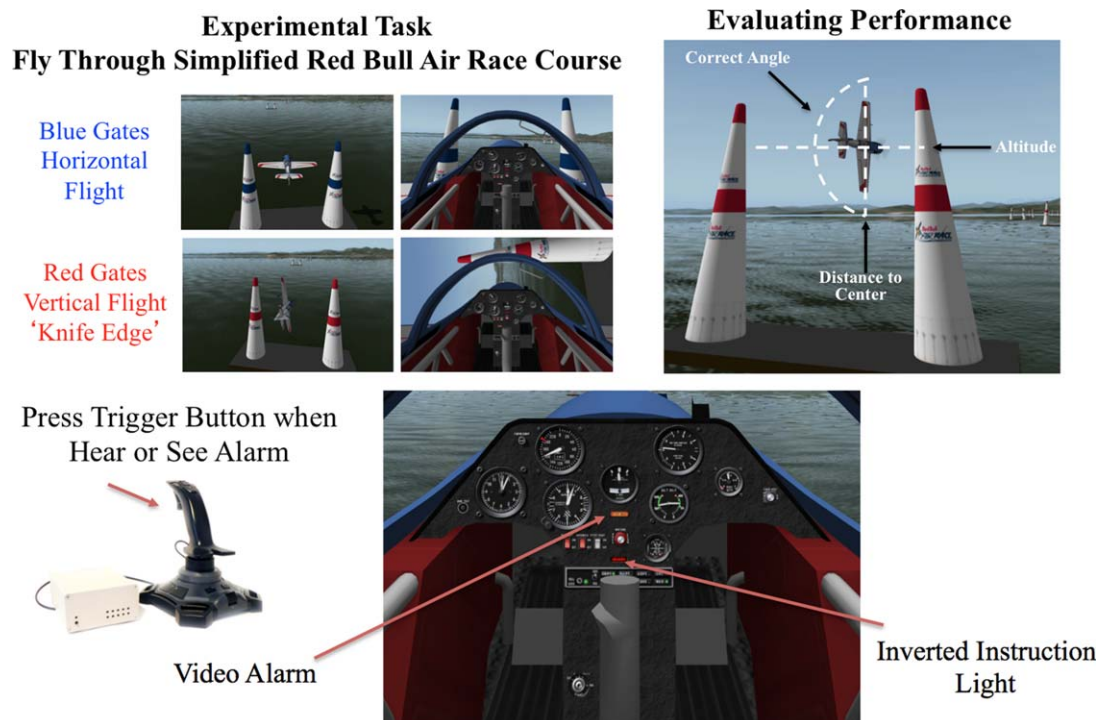


Figure 1.
The Red Bull flying task.

It is hypothesized that inattentional deafness (defined by audio misses > audio hits) will be signified by greater activity in brain regions generally involved in attentional bottleneck processing including the lateral prefrontal cortex, IFG, SMFC, and insula. It follows that these same attentional bottleneck regions will also be active to a greater extent when the flying task is difficult (gates missed > gates passed). It is maintained that the activation in these areas represents processes used to selectively attenuate modality specific perception under excessive load conditions. It is therefore hypothesized that these attentional bottleneck regions may suppress selective attentional processes that afford perceptual enhancement (manifest in a reduction in effective connectivity from these regions to auditory cortex for audio misses relative to hits).

METHODS

Participants

The participants were 15 Japanese right-handed adults (5 females, 10 males) aged 20–25 years (mean = 21.82, SE = 0.366). There were originally 22 participants but seven of them were eliminated from the study because they did not meet the behavioral performance criterion for the audio and or video perception task required for inclusion (see below for details on criterion for inclusion). All participants

reported prior experience with first person video games such as driving games and flight simulation. They all reported having normal hearing and the vision was corrected to normal if needed. The experimental procedures were approved by the NICT Human Subject Review Committee and were carried out in accordance with the principles expressed in the WMA Declaration of Helsinki.

Experimental Task and Procedure

In this fMRI experiment, we explore the brain regions active during the occurrence of inattentional deafness using a flight simulation task (using X-Plane Version 9.7 Laminar Research). The participants fly through a simplified Red Bull Air Race course (using a joystick to control elevator and aileron deflections resulting in pitch and roll) passing through a number of gates and at the same time push a button on the joystick to the presence of audio and video alarms. The Red bull Air Race course (objects for X-Plane developed by Fred Ider) was the same as that used in Callan et al. [2012]. The flying task involved passing through a number of colored gates, each composed of two pylons, at the correct altitude, and correct orientation angle (nominally horizontal for blue gates and vertical for red gates unless the instructions were inverted) (Fig. 1). The aircraft used in the simulation was a Sukhoi SU-26 with a wingspan of 7.8 m traveling at an average speed of

F1

320 km/h (173 knots). The distance between the pylons was 14 m and the passing altitude was from 11.5 to 21.5 m. If the plane was below 5 m (counted as a crash), above 70 m, or 200 m away from the course, the plane would be reset to the start of the course. In addition, after flying through the ninth and final gate of the course, the plane would be reset to the start of the course. Participants practiced the flying task only for about 1 h ~1–2 weeks before the fMRI experiment.

A first-person view was presented from within the cockpit such that the bottom half of the display was the instrument panel of the plane and the top part of the display was the view of the world through the cockpit canopy (Fig. 1). In real flight, pilots must maintain visual attention to both the instruments and to the world outside the plane. To simulate these perceptual demands, we presented a light on the instrument panel (Fig. 1) that would inform whether the orientation instruction in which they were to fly through the gates was inverted (light on means blue gate is now vertical flight and red gate is now horizontal flight). The inverted instruction light had a 33% chance of being toggled after each gate was passed.

The audio alarm was a short 250 ms beep sound (composed of harmonics at 600 and 1000 Hz) played loud enough to be clearly audible even within the fMRI scanner. The video alarm was an additional light on the instrument panel displayed for 250 ms (Fig. 1).

Participants were instructed to focus on the difficult piloting task and to maximize the number of gates they would pass during the length of each session while avoiding crashing. They were also instructed to press the button on the joystick as fast as possible when they noticed an audio or video alarm (see Supporting Information, Video 1 for example of experimental task). After the experiment, the participants were asked to rate their perceived difficulty of the experiment (including the flying and perceptual tasks) on a 10-point scale, with 1 being very easy and 10 being very difficult.

fMRI Data Collection, Preprocessing, and Analysis

The fMRI experiment consisted of four 16 min experimental sessions using a Siemens Trio 3 T scanner located at the Center for Information and Neural Networks. A multiband EPI sequence was used with a TR of 1.7 s and a $3 \times 3 \times 3$ mm voxel resolution across the entire brain (50 axial slices). A total of 567 scans were collected for each experimental session.

Before and after collection of the experimental sessions the participants had an 8 min session (290 scans) in which resting-state activity was collected (analysis of the resting-state sessions was not included in this study). After the final resting-state session, a T1 anatomical MRI scan with $1 \times 1 \times 1$ mm voxel resolution was acquired.

Video was presented to the participant by a projector to a mirror behind the head coil that could be viewed by a mirror mounted on the head coil. Audio was presented by MR-compatible headphones (Hitachi Advanced Systems' ceramic transducer headphones; frequency range 30–40,000 Hz, ~20 dB SPL passive attenuation). The background sound of the airplane by the flight simulator (engine, propeller, wind) was constantly playing in the background in addition to the audio alarms. The alarm stimulus composed of frequencies at 600 and 1000 Hz was presented at approximately 90 dBA (recorded using Bruel & Kjaer sound level meter type 2250-S). The background engine propeller sound was presented at ~80 dBA with the greatest power at 120 Hz with some reduced power at 100, 155, 206, 236, 275, 310, 350, and 466 Hz (recorded using Bruel & Kjaer sound level meter type 2250-S). The maximum sound pressure level of the multiband EPI sequence used in this study recorded inside the bore was 95 dBA with a dominant peak at 700 Hz and a lesser one at 2200 Hz (recorded using microphone on Opto Acoustics MRI compatible noise canceling headphone). The Hitachi Advanced Systems' headphones used in this study provided ~20 dB of passive attenuation. This would place the scanner noise at ~75 dBA about 15 dB lower than the level at which the alarm stimuli were presented.

The audio alarms were played ~10 dB higher in amplitude than the background airplane noise. The experiment consisted of a Red Bull flying task as explained above simultaneously together with an audio and video alarm detection task. A single occurrence of the Red Bull flying task was 2 min long and was repeated 5 times within a session. An auditory or visual alarm was pseudorandomly presented every 7, 8, or 9 s. During the Red Bull Flying task, there were 35 audio and 35 video alarms within a single session.

An additional flying task in which the participant flew straight (flying straight task) at a higher altitude above the gates without going through them while simultaneously carrying out the audio and video alarm detection task (1 min long) was repeated 5 times within a session after each Red Bull flying task. There were 17 or 18 audio and video alarms within a single session of the flying straight task. The reason for the lower number of stimuli for the flying straight task relative to the Red Bull flying task (35 audio and 35 video) was based on time constraints to keep the total time in the scanner under 90 min and to maximize the number of trials in the experimental condition of interest (Red Bull flying task). The instructions for the task were presented by a symbol presented on the screen for 2 s in between each task. An arrow pointing up signified the Red Bull flying task and an equal sign denoted the flying above the gates task. As a result of the majority of participants not following the task rules properly during the flying straight task (they continued to implement the Red Bull flying task), events from this task were not used in any of the experimental contrasts of interest conducted in this study. Owing to the focused attention on the Red Bull

◆ Neural Signature of Inattentional Deafness ◆

flying task and the rapidity of the transition between tasks, it is possible that most of the participants failed to initiate the flying straight task in a timely manner because they did not notice the instruction symbol given. The audio and video alarms presented during the flying straight task were modeled as events of noninterest to ensure that resultant brain activity did not interfere with general linear model GLM analysis of events from the Red Bull flying task.

Preprocessing of the fMRI scans was carried out using programs within SPM8 (Wellcome Department of Cognitive Neurology, UCL). Images from the four experimental sessions were realigned, unwarped, spatially normalized to a standard space using a template EPI image ($2 \times 2 \times 2$ mm voxels), and were smoothed using an $8 \times 8 \times 8$ mm FWHM Gaussian kernel.

As a result of extremely poor audio and/or video behavioral performance on some of the sessions, for a number of participants, a criterion was established for a session to be included in the SPM analysis. To ensure that participants were engaged in the dual tasks of flying the airplane and perceiving the alarms (audio and video) and guarantee a reasonable number of hit/miss trials for statistical analysis, a minimum criteria was set at 20% hit rate (for both audio and video conditions) for a session to be included in the analysis. The mean hit rate over the 88 sessions ($22 \text{ participants} \times 4 \text{ sessions}$) was 53.3% ($SE = 3.6\%$) for audio alarms and 63.1% ($SE = 2.3\%$) for video alarms. To obtain at least 15 participants meeting the minimum performance criteria, it was required that only two sessions be included out of the four runs for each participant. In the case of more than 2 sessions meeting, the inclusion criteria the sessions with the least amount of crashes were selected. In addition to the 5 participants eliminated from the analysis because they did not have at least two sessions fitting the performance inclusion criteria, 2 additional participants were eliminated from the analysis for not having any audio and/or visual misses in at least two sessions (resulting in a nonexistent “miss” experimental condition). The mean hit rate over the four sessions for the 5 participants not included in the study because of poor performance was 8.6% ($SE = 2.4\%$) for audio alarms and 66.0% ($SE = 4.4\%$) for the video alarms. The mean hit rate over the four sessions for the 2 participants not included in the study because of too good performance was 99.3% and 98.6% for audio alarms and 93.6% and 87.1% for the video alarms. Because many of the sessions that did not meet the inclusion criteria had 0 hits (and in the case of great performance 0 misses), they could not be included in the GLM and were therefore removed from further analysis. For this reason, only 2 sessions were included in the analysis for all participants.

Regional brain activity for the various conditions of the two selected sessions for each participant was assessed using a general linear model GLM employing an event-related design. To account for lag in the blood oxygenation level dependent

(BOLD) response in relation to the various events, the canonical hemodynamic response function HRF was convolved with their onset and represented in the GLM (see below for a list of events that were modeled). Autoregression was used to correct for serial correlations. High pass filtering (cutoff period 128 s) was carried out to reduce the effects of extraneous variables (scanner drift, low frequency noise, etc.). The participants were instructed to keep their body as still as possible to reduce the degree of head and body movement artifacts during the flying tasks. The use of a strap on the forehead and cushions around the head were also used to immobilize the head. The joystick was placed next to the participant in a manner such that minimal movement of the hand and wrist was required to control the continuous movement of the airplane to reduce potential body movement related artifacts. In addition, the six realignment parameters were included in the general linear model GLM for all analyses as regressors of noninterest to account for biases in head movement correlations present during the experimental conditions.

For each participant, we conducted fixed-effect SPM analyses using the GLM. The variables of interest entered into the analyses as events of zero duration were all within the Red Bull flying task and included audio hits, audio misses (audio alarms), video hits, video misses (video alarms), gates passed, and gates missed (performance on the Red Bull flying task). In the final fixed effect SPM analysis, each participant's data was composed of 2 sessions, each with 567 volumes including events for 35 audio alarms and 35 video alarms (divided into hits and misses), and the gates passed and missed, all from the Red Bull flying task, and dependent on the participant's performance. Variables of noninterest were also entered into the analyses consisting of the following events with zero duration: audio and video alarms on the flying straight task, button responses, and crashes. The instruction between alternating flying tasks were also entered into the analyses as a variable of noninterest with duration of 2 s. The volumes from the flying straight task could not simply be removed from the data because it would cause temporal discontinuities that would be problematic for SPM analysis utilizing convolution of the time-course data with the HRF and interfering with the autoregression and high pass filtering preprocessing steps used to remove artifacts.

The following analyses were conducted to test our hypotheses:

- (audio misses > audio hits): Contrasting audio misses and audio hits during the Red Bull flying task assessed differences in active neural processes that may be related to inattentional deafness. While the brain regions identified during the audio misses greater than audio hits contrast are sites potentially related to inattentional deafness, they are likely generally involved with selective attentional modulation of perception under high workload conditions.
- (audio hits > audio misses): Greater relative activity for audio hits over misses assessed whether there was

a suppression of auditory activity that may be related to inattentional deafness.

- (audio misses > audio hits) – (video misses > video hits): Although the audio alarms presented were identical between hits and misses controlling for stimulus-based confounds the presence of a button press and the associated decision making processes leading to a motor command during a hit may pose as a potential confound. To ensure that the results were not due to the occurrence of a button response for audio hits that is not present for audio misses, the contrast of (audio misses > audio hits) – (video misses > video hits) was assessed. The video conditions contain the same relationship with regards to the button response, therefore, this potential confound can be controlled for by this contrast.
- (Gates missed > gates passed): Poor flying performance was assessed by this contrast.
- (Gates passed > gates missed): Good flying performance was assessed by this contrast.
- Conjunction of (audio misses > audio hits) and (Gates missed > gates passed): Brain regions potentially involved with an attentional bottleneck in which performance is degraded was assessed by the intersection (conjunction) of activity present for both the contrast of (audio misses > audio hits) and (gates missed > gates passed). It is hypothesized that even though the audio perceptual task and the Red Bull flying task are considerably different, there are overlapping attentional processes necessary for both that will be excessively active when performance is poor for either task because these regions are limited in the extent that they can process multiple tasks. Based on previous studies [Dux et al., 2006; Szameitat et al., 2016; Tombu et al., 2011]), greater activity is predicted in these attentional bottleneck brain regions under high workload multitasking situations that are associated with degraded performance.
- Psychophysiological interaction (PPI) analysis for the audio misses > audio hits contrast: A connectivity analysis using psychophysiological interaction for the contrast of audio misses relative to hits was used to evaluate the relationship between activity in these attentional bottleneck regions and the auditory processing in relevant brain regions in the STG and MTG.

Random effects analyses were conducted across participants for the contrasts of interest given above using *t* tests within SPM8. Correction for multiple comparisons ($P < 0.05$) across the entire brain was carried out using the false discovery rate (FDR) for voxel-wise analyses. Cluster level correction for multiple comparisons was conducted using Monte-Carlo simulation of the brain volume to define a voxel contiguity threshold at an uncorrected significance level of $P < 0.005$ using the AFNI [Cox, 1996] 3dClustSim program. This program has been revised to address

TABLE I. Inattentional deafness audio misses relative to audio hits

Brain region	MNI coordinates <i>x, y, z</i>	<i>T</i>	Cluster size
SMFC Pre-SMA BA6,8	6,30,52	4.81	312
SMFC Pre-SMA BA6,8	12,22,68	4.03	
IFG BA44,45	54,14,4	4.82	333
IFG BA47,45	48,28,-10	4.15	
IFG BA47	52,18,-6	3.92	

Brain regions showing significant differential activity for audio misses > audio hits corrected for multiple comparisons at the cluster level ($P < 0.05$) within the frontal ROI (16,535 voxels) using Monte-Carlo simulation (corrected cluster extent threshold = 140 contiguous voxels over an uncorrected significance threshold of $P < 0.005$). BA = Brodmann area; SMFC = superior medial frontal cortex; pre-SMA = pre-supplementary motor area; IFG = inferior frontal gyrus. Negative “*x*” MNI coordinates denote left hemisphere and positive “*x*” values denote the right hemisphere activity.

problems with cluster-level correction for multiple comparisons identified in Eklund et al. [2016]. Noise smoothness values using a spatial autocorrelation function were calculated using 3dFWHMx AFNI [Cox, 1996] program using the residual mean square image and the brain mask image from the random effects SPM analyses. Using 3dClustSim, 10,000 Monte-Carlo simulations were used to determine cluster size threshold correcting for multiple comparisons.

Region of interest (ROI) analyses were carried on in brain regions thought to be involved with the attentional bottleneck including the lateral prefrontal cortex, inferior frontal gyrus (IFG), and superior medial frontal cortex SMFC [Dux et al., 2006; Tombu et al., 2011]. The ROI masks were constructed using the WFU PickAtlas Tool Version 2.5.2.

The attentional bottleneck ROI was defined using the intersection of automated anatomical labeling (AAL) regions located in the frontal middle cortex, the frontal inferior operculum, the inferior frontal gyrus, the frontal superior medial frontal cortex (including pre-SMA), and the prefrontal portion of the SMA with the Brodmann area (BA 9, 44, 45, 46, and 47) defined regions (using a dilation coefficient of 4). This allowed for a smaller and more theory-driven ROI.

The ROI used for the PPI analysis in the temporal lobe auditory processing regions consisted of Heschl’s gyrus the superior temporal gyrus (STG), and the middle temporal gyrus (MTG).

For the ROI analysis involving the visual motion processing area V5, a small volume correction for multiple comparisons (using a sphere with a radius of 10 mm) was made using the coordinates given in Zeki et al. [2003] (MNI coordinates: right 53,-71,-4; left -49,-77,-1). The V5 region was chosen as the visual region of

Inattentional Deafness Audio Misses > Audio Hits

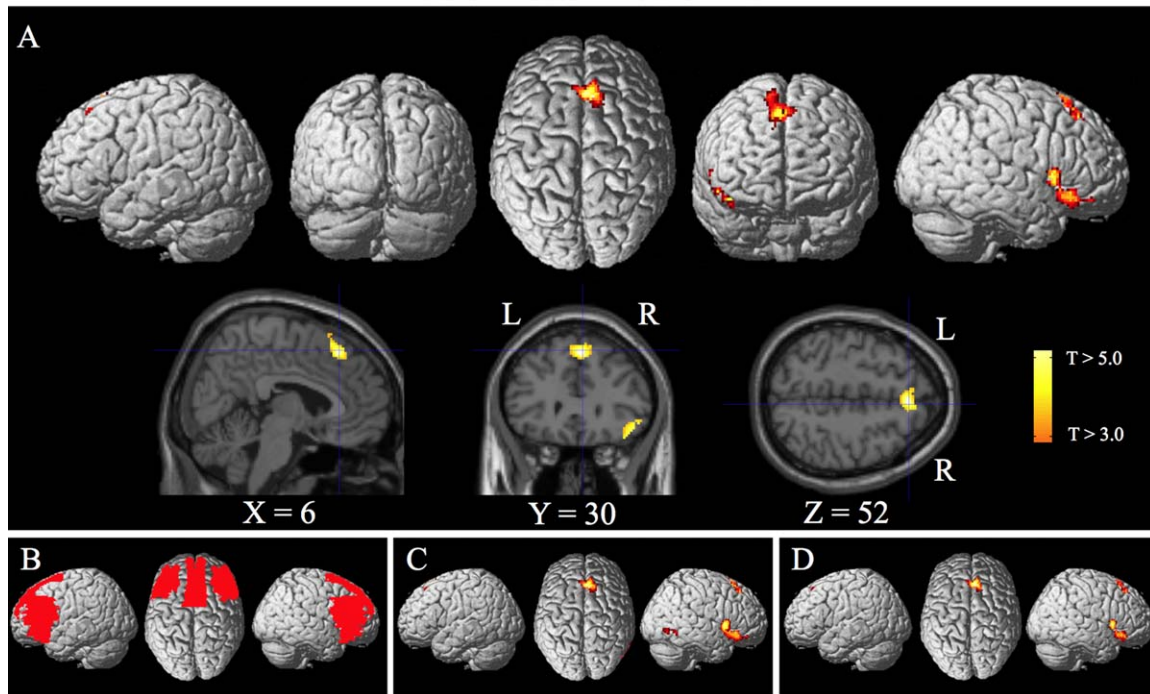


Figure 2.

Brain activity for the contrast investigating inattentional deafness (audio misses > audio hits). (A) Significant differential activity in the IFG and the SMFC/Pre-SMA for the audio misses > audio hits contrast ($P < 0.05$ cluster level corrected for multiple comparisons within frontal ROI) rendered on the surface of the cortex (Top) and in selected anatomical MRI slices with corresponding MNI coordinates (Bottom). (B) Voxels included in the frontal ROI rendered on the surface of the cortex. (C) Differential activity across the entire brain using the same uncorrected voxel wise threshold as in Figure 2A of $P < 0.005$ (voxel

extent threshold = 30 voxels). (D) To ensure that the results in 2A are not confounded by unequal number of stimuli in the miss and hit conditions, miss rate was used as a covariate of noninterest in the contrast of audio misses > audio hits. Significant differential activity ($P < 0.05$ cluster level corrected for multiple comparisons within frontal ROI) was found in the same brain regions to be almost identical to those given in 2A. L = Left; R = Right; IFG = Inferior Frontal Gyrus; SMFC = superior medial frontal cortex; Pre-SMA = Pre-supplementary motor area.

interest because of the dynamic nature of the flying task requiring tracking of objects in a moving optic flow field.

Activated brain regions were identified using the SPM Anatomy Toolbox v1.8 [Eickhoff et al., 2005] and Talairach Client after using the Matlab mni2tal function to transform from the MNI to the Talairach coordinate system.

RESULTS

Behavioral Results

The participants rated the difficulty of the experiment (both the flying and perceptual tasks combined) at an average of 8.6 (SE = 0.26) out of 10 (with 1 being very easy and 10 being very difficult) with a range from 7 to 10. The performance on the perceptual tasks of detecting the

presence of an alarm (visual or auditory) was computed for each participant.

For auditory alarms, the mean performance across participants for the two sessions combined was 67.9% hits (SE = 4.7%) and 32.1% misses (SE = 4.7%). The difference between audio hits and misses was statistically significant (Wilcoxon Signed Rank Test, $P < 0.002$, two-tailed, $n = 15$). For isual alarms, the mean performance across participants for the two sessions combined was 54.9% hits (SE = 4.9%) and 45.1% misses (SE = 4.9%). The difference between video hits and misses was not statistically significant (Wilcoxon Signed Rank Test, $P > 0.05$, two-tailed, $n = 15$). The difference between audio misses (32.1%, SE 4.7%) and video misses (45.1%, SE 4.9%) was statistically significant (Wilcoxon Signed Rank Test, $P < 0.009$, two-tailed, $n = 15$).

The results for the flying performance on the Red Bull Air Race course was assessed by measuring whether the

TABLE II. Inattentional deafness specific to auditory (audio miss–audio hit) relative to (video misses–video hits)

Brain region	MNI coordinates <i>x, y, z</i>	<i>T</i>	Cluster size
SMFC Pre-SMA BA6,8	−2,24,58	3.98	161
SMFC Pre-SMA BA6,8	6,24,60	3.34	
IFG BA47	42,30,−18	4.22	159
IFG BA47	48,24,−16	4.04	
IFG BA47	52,18,−6	3.09	

Brain regions showing significant differential activity for the contrast of (audio misses > audio hits) relative to (Video Misses > Video Hits) corrected for multiple comparisons at the cluster level ($P < 0.05$) within the frontal ROI (16535 voxels) using Monte-Carlo simulation (corrected cluster extent threshold = 143 contiguous voxels over an uncorrected significance threshold of $P < 0.005$). BA = Brodmann area; SMFC = superior medial frontal cortex; pre-SMA = pre-supplementary motor area; IFG = inferior frontal gyrus. Negative “*x*” MNI coordinates denote left hemisphere and positive “*x*” values denote right hemisphere activity.

plane passed through the gate at the correct altitude (no higher than the cones) without hitting either of the two cones. The angle at which the plane flew through the gate was not taken into account when computing the performance due to the difficulty of the task for most participants. Over the two sessions, the participants passed an average of 87.2 gates ($SE = 11.46$) and missed an average of 178.9 gates ($SE = 10.53$). The difference between the number of gates passed and gates missed was statistically

significant (Wilcoxon Signed Rank Test, $P > 0.002$ two-tailed, $n = 15$).

To explore the relationship between audio misses and difficulty on the flying task, an analysis was conducted looking at the percentage of gates missed on the flying task for audio misses versus audio hits. For audio misses, 65.1% of them occurred when a gate was missed on the flying task compared to 52.2% for audio hits. A Wilcoxon Signed Rank Test indicated a significant difference in the percent of gates missed on the flying task between audio misses and hits ($P < 0.001$ two-tailed, $n = 15$). Because of the continuous nature of the flying task, the audio alarm was required to occur within 2 s before or after the gate to be included in the analysis.

Brain Imaging Results

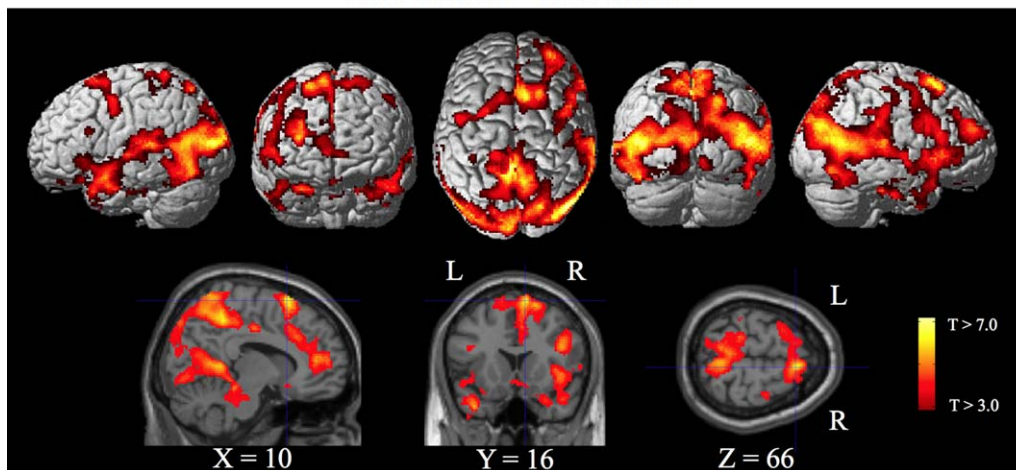
Perceptual tasks

The results for audio misses greater than audio hits are given in Figure 1 and Table I. An ROI analysis was conducted within frontal brain regions (see methods section for description of how ROI was defined) thought to be potentially involved with an attentional bottleneck. The results of this analysis revealed significantly greater activity for audio misses over hits ($P < 0.05$ cluster level corrected) in the IFG and in the SMFC/pre-SMA (Fig. 2A and Table I). The results are corrected within the frontal ROI (consisting of 16,535 voxels) for multiple comparisons at the cluster level ($P < 0.05$) using Monte-Carlo simulation (corrected cluster extent threshold >157 contiguous voxels over an uncorrected significance threshold of $P < 0.005$).

T1

F2

Flying Performance Gates Missed > Gates Passed

**Figure 3.**

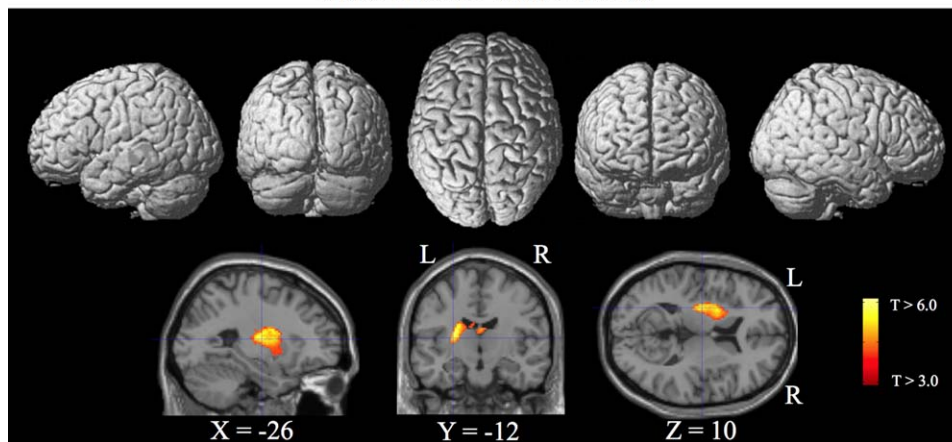
Brain activity for poor performance on the Red Bull flying task (gates missed > gates passed). Significant differential activity for the gates missed > gates passed contrast ($P < 0.05$ FDR voxel level corrected across entire brain) rendered on the surface of the cortex (Top) and in selected anatomical MRI slices with corresponding MNI coordinates (Bottom). L = left; R = right.

TABLE III. Flying performance gates missed > gates passed

Brain region	MNI coordinates <i>x, y, z</i>	<i>T</i>	Cluster size
Parahippocampal Gyrus BA36	36, -24, -30	7.77	38286
Posterior Cingulate BA30	24, -56, 10	7.75	
Calcarine Gyrus BA17,18	22, -52, 8	7.48	
Calcarine Gyrus BA17,18	-18, -62, 6	5.19	
Paracentral Lobule BA5	-4, 44, 54	7.25	
Fusiform Gyrus BA37	-36, -50, -20	7.23	
Fusiform Gyrus BA37	-30, -50, -16	7.00	
Precuneus BA7	6, -54, 54	5.40	
STG, Transverse Temporal Gyrus BA41,22	48, -26, 10	6.70	
Superior Occipital Gyrus BA19	44, -80, 26	6.68	
MT hOC5(V5)	44, -78, 16	6.13	3631
MT hOC5(V5)	-44, -68, 16	5.81	
MTG BA21	-44, 2, -22	5.12	
STG, Transverse Temporal Gyrus BA41,22	-50, -24, 10	4.79	
IFG BA44,45	44, 16, 24	4.66	
IFG BA9,6,44,45	42, 6, 28	4.64	
IFG BA47	44, 17, -4	4.40	
Insula BA13	36, 22, 2	4.27	
Superior Frontal Gyrus BA6	20, 20, 60	5.86	925
SMA BA6	10, 16, 66	5.77	
Anterior Cingulate BA32	12, 44, 12	4.96	
Middle Cingulate BA32	6, 26, 34	4.98	
Middle Frontal Gyrus BA10	32, 50, 16	4.88	
Superior Frontal Gyrus BA10	30, 56, 22	4.15	
Middle Frontal Gyrus BA9	28, 36, 28	3.12	
Middle Cingulate Gyrus BA24	8, -14, 40	4.54	159
Middle Cingulate Gyrus BA24	-6, -10, 42	3.57	
Anterior Cingulate BA32	-4, 24, -8	3.95	
Cerebellum Lobule IX	20, -54, -40	3.52	
Orbital Gyrus BA11	0, 42, -20	3.19	
Middle Frontal Gyrus BA46	-42, 18, 24	3.11	
Postcentral Gyrus BA3	36, -26, 42	2.94	
Postcentral Gyrus BA3	-36, -36, 64	2.82	

Brain regions showing significant (pFDR < 0.05 correct for multiple comparisons) differential activity for the contrast of Gates Missed > Gates Passed. An arbitrary spatial extent threshold of 25 voxels was used to avoid reported activity in very small clusters). BA = Brodmann area; STG = superior temporal gyrus; MT = middle temporal; hOC5(V5) = human visual motion processing area V5; IFG = inferior frontal gyrus; SMA = supplementary motor area. Negative “x” MNI coordinates denote left hemisphere and positive “x” values denote right hemisphere activity.

Flying Performance Gates Passed > Gates Missed

**Figure 4.**

Brain activity for good performance on the Red Bull flying task (gates passed > gates missed). Significant differential activity for the gates passed > gates missed contrast ($P < 0.05$ cluster-level corrected across entire brain) rendered on the surface of the cortex (Top) and in selected anatomical MRI slices with corresponding MNI coordinates (Bottom). L = left; R = right.

TABLE IV. Flying performance gates passed > gates missed

Brain region	MNI coordinates <i>x, y, z</i>	<i>T</i>	Cluster size
Putamen	-24,-10,18	6.59	1282
Putamen	-26,-12,10	5.61	
Caudate	-16,-24,20	5.51	

Brain regions showing significant differential activity for the contrast of Gates Passed > Gates Missed corrected for multiple comparisons at the cluster level ($P < 0.05$) over the entire brain (205,393 voxels) using Monte-Carlo simulation (corrected cluster extent threshold = 761 contiguous voxels over an uncorrected significance threshold of $P < 0.005$). Negative “*x*” MNI coordinates denote left hemisphere and positive “*x*” values denote right hemisphere activity.

The ROI mask for the frontal brain regions is shown in Figure 2B. The results of the contrast for audio misses over hits across the entire brain at an uncorrected threshold of $P < 0.005$ are given in Figure 2C to show that activation were mainly specific to frontal regions. To ensure that the results were not due to unequal numbers of misses and hits across participants the miss rate was used as a covariate of noninterest in the analysis of audio misses > audio hits (Fig. 2D). The results (Fig. 2D) are essentially identical to those given in Figure 2A suggesting that there was no confound based on unequal numbers of misses and hits in the analyses. The ROI analysis within the right V5 visual motion processing area showed a significant difference using a small volume correction for multiple comparisons for the audio

misses > audio hits contrast ($P < 0.05$ FWE; $T = 3.86$, 37 voxel cluster).

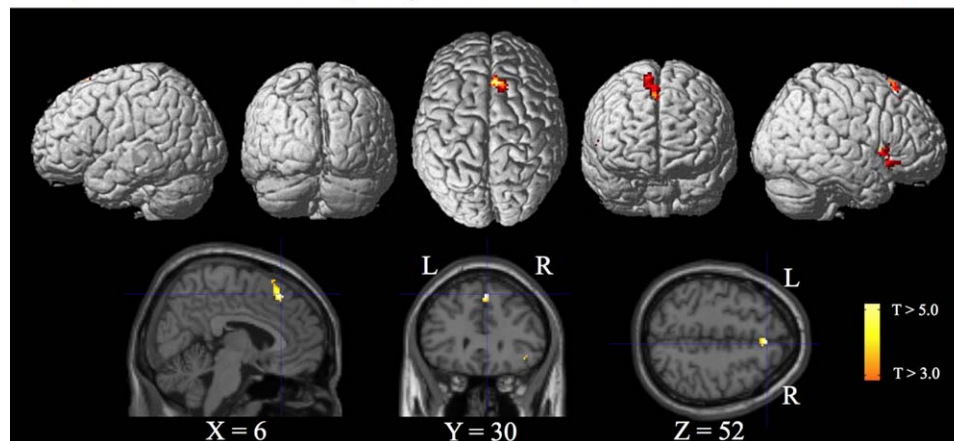
To ensure that these results were not due to the presence of a button response for hits but not for misses, the following contrast was conducted (Audio Misses > Audio Hits) – (Video Misses > Video Hits). The results of this analysis in the frontal ROI revealed significant activity ($P < 0.05$ cluster level corrected) in the same two regions, (the IFG and the SMFC/pre-SMA, see Table II). The results were corrected for multiple comparisons within the frontal ROI at the cluster level ($P < 0.05$) using Monte-Carlo simulation (corrected cluster extent threshold greater than 159 contiguous voxels over an uncorrected significance threshold of $P < 0.005$).

There were no significant differences when correcting for multiple comparisons across the whole brain or within the defined frontal and V5 ROIs for the contrasts of audio hits > audio misses, video misses > video hits, or video hits > video misses. The contrasts of audio hits > audio misses and the contrast of gates missed > audio hits were further assessed within the STG/MTG ROI. However, no significant differential activity was found for these contrasts when correcting for multiple comparisons within this ROI.

Flying task

The results on the flying task for poor performance defined by the contrast of gates missed > gates passed are given in Figure 3 and Table III. Widespread significant differential activity ($P < 0.05$ pFDR corrected) is present in

Attentional Bottleneck (Audio Miss > Audio Hit) Conjunction with (Gates Missed > Gates Passed)

**Figure 5.**

Brain regions potentially involved with attentional bottleneck. The intersection (Conjunction) of significant differential activity for the audio misses > audio hits contrast (Fig. 2) and the gates missed > gates passed contrast (Fig. 4) rendered on the surface of the cortex (Top) and in selected anatomical MRI slices with

corresponding MNI coordinates (Bottom). L = left; R = right. The IFG and the SMFC/Pre-SMA show overlapping activity for both contrasts. L = left; R = right; IFG = inferior frontal gyrus; SMFC = superior medial frontal cortex; Pre-SMA = pre-supplementary motor area.

♦ Neural Signature of Inattentive Deafness ♦

T4

TABLE V. Attentional bottleneck (audio miss > audio hit) conjunction with (gates missed > gates passed)

Brain region	MNI coordinates		T	Cluster size
	x, y, z			
SMFC Pre-SMA BA6,8	6,30,52		4.81	144
SMFC Pre-SMA BA6,8	12,22,68		4.03	
IFG BA44,45	52,14,4		4.74	76
IFG BA47	52,18,-6		3.92	

Brain regions showing significant differential activity for both the contrast of audio misses > audio hits (Fig. 1 and Table I) and the contrast of gates missed > gates passed (Fig. 2 and Table III). BA = Brodmann area; SMFC = superior medial frontal cortex; pre-SMA = pre-supplementary motor area; IFG = inferior frontal gyrus. Negative “x” MNI coordinates denote left hemisphere and positive “x” values denote right hemisphere activity.

cortical areas including the IFG, premotor cortex, prefrontal cortex, pre-SMA, superior temporal gyrus/sulcus, visual motion processing area V5 (middle temporal MT), superior/middle occipital gyrus, precuneus, cingulate cortex, and cerebellum (Fig. 3 and Table III).

The analysis of good piloting performance defined by the contrast of gates passed > gates missed revealed significant ($P < 0.05$ cluster level corrected) differential activity in the basal ganglia (Fig. 4 and Table IV). The results are

F4

corrected across the entire brain (consisting of 205,393 voxels) for multiple comparisons at the cluster level ($P < 0.05$) using Monte-Carlo simulation (corrected cluster extent threshold >761 contiguous voxels over an uncorrected significance threshold of $P < 0.005$).

Attentional bottleneck

Brain regions potentially involved with an attentional bottleneck were defined by a conjunction of activities related to poor performance on the audio perceptual task (audio misses > audio hits) and poor performance on the flying task (gates missed > gates passed). Overlapping activity for these two contrasts is present in both the IFG and the SMFC/pre-SMA (Fig. 5 and Table V), which were the regions associated with auditory misses. The V5 ROI analysis was also found to show overlapping activity for both of these contrasts (peak voxel for audio misses > audio hits: 58, -68, -4, $T = 3.86$; peak voxel for gates missed > gates passed: 50, -66, 4, $T = 4.56$).

F5 T5

Psychophysiological Interaction Analysis

To assess the potential effects that an attentional bottleneck may have on auditory processing, psychophysiological interaction PPI analyses were carried out for the contrast of audio misses > audio hits from the IFG and

**Psychophysiological Interaction Analysis
For the Contrast of Audio Misses > Audio Hits
Connectivity from IFG to the STG/MTG**

**Figure 6.**

Effective connectivity from attentional bottleneck region in IFG to auditory processing regions in STG/MTG. Significant negative differential connectivity ($P < 0.05$ cluster level corrected in STG/MTG ROI) found in the STG using a psychophysiological interaction analysis for the contrast of audio misses > audio hits rendered on the surface of the cortex (Top) and in selected anatomical MRI slices with corresponding MNI coordinates

(Bottom). The very left side of the figure shows the MNI coordinates and the rendered brain image of the location of the seed voxel in the IFG used for the psychophysiological interaction analysis. L = left; R = right. IFG = inferior frontal gyrus; STG = superior temporal gyrus; MTG = middle temporal gyrus; L = left; R = right; IFG = inferior frontal gyrus.

TABLE VI. Psychophysiological interaction analysis for the contrast of audio misses > audio hits connectivity from IFG to the STG/MTG

Brain region	MNI coordinates <i>x, y, z</i>	<i>T</i>	Cluster size
STG BA22	48, -6, -6	5.25	213
STG BA22	48, -12, -8	4.43	
STG BA22	58, 8, -6	3.5	

Significant connectivity from the IFG (seed voxel MNI 52,18,-6) to the STG/MTG ROI related to the contrast of audio misses > audio hits corrected for multiple comparisons at the cluster level ($P < 0.05$) using Monte-Carlo simulation (corrected cluster extent threshold = 110 contiguous voxels over uncorrected significance threshold of $P < 0.005$). Negative *T* values denote that there was significantly less connectivity for audio misses relative to audio hits. BA = Brodmann area; STG = superior temporal gyrus; MTG = middle temporal gyrus; IFG = inferior frontal gyrus. Negative “*x*” MNI coordinates denote left hemisphere and positive “*x*” values denote right hemisphere activity.

pre-SMA to the superior and middle temporal gyrus STG/MTG bilaterally (regions involved with auditory processing). Significant negative ($P < 0.05$ cluster level corrected) task related connectivity for audio misses > audio hits was present from the IFG (seed voxel at 52, 18, -6) to the temporal lobe in the STG (Fig. 6 and Table VI). The results are corrected within the STG/MTG ROI (consisting of 15,832 voxels) for multiple comparisons at the cluster level ($P < 0.05$) using Monte-Carlo simulation (corrected cluster extent threshold > 110 contiguous voxels over an uncorrected significance threshold of $P < 0.005$). There was no significant differential connectivity found by PPI analysis from the pre-SMA (seed voxel at 6,30,52) within the STG/MTG ROI.

DISCUSSION AND CONCLUSION

This study was aiming to identify for the first time the neural substrates responsible for the phenomenon of inattentional deafness by contrasting alarms that were not perceived (misses) versus alarms that were perceived (hits). We implemented an ecological simulated flight experiment in an fMRI design able to elicit this phenomenon.

The simulated piloting task inspired from the Red Bull Air Race and involving auditory and visual alarms was judged by the participants as having a high level of difficulty (rated as 8.6 out of 10), resulting in poor flying performance, as they missed a large number of the gates on average. In addition, as a result of the high level of load generated by this dynamic task [MacDonald et al., 2011; Raveh et al., 2015], the participants failed to signal a large part (32.1%) of the auditory alarms presented during the session.

The results of the fMRI analyses, when contrasting auditory misses relative to auditory hits, revealed significantly greater activity in the SMFC/pre-SMA and the right IFG.

This finding was also present when considering the interaction with the contrast between visual hits and misses to verify that the measured activations did not correspond to the presence of a button press. This result suggests that these regions are associated with the phenomenon of attentional deafness. It is in accordance with a previous investigation that found greater activations of frontal cortical areas with increasing levels of load [Culham et al., 2001]. A likely explanation of the link between these activations and inattentional deafness is that the greater activity measured in frontal regions would be the result of greater application of top-down attenuation of perceptual processes in high load conditions [Lavie et al., 2014].

Accordingly, the conjunction analysis showing common activity for inattentional deafness occurrence (audio misses > hits) and poor user performance (gates missed > gates passed) revealed the activation of the SMFC/pre-SMA and IFG in the attentional bottleneck involved in the decrease of performance at both the perceptual and piloting tasks. These regions have previously been identified during laboratory tasks as sites representing a central attentional bottleneck [Dux et al., 2006; Szameitat et al., 2016; Tombu et al., 2011]. The limitation of these regions in the extent they can process multiple tasks explains the degraded performance associated with their activation.

This attribution of central attentional bottleneck functions to the SMFC/pre-SMA and IFG was also reinforced in our findings by the decrease of reduced effective connectivity from the IFG to the primary auditory cortex in the STG during inattentional deafness. Therefore, similar to the mechanisms identified as potentially responsible for inattentional blindness [Lavie et al., 2014], the involvement of the brain regions associated with the attentional bottleneck may suppress selective attentional processes that afford perceptual enhancement.

Additionally, the reduced connectivity from the IFG to the auditory processing regions of the STG supports the idea that the activation of the regions of the attentional bottleneck drives an attenuation of early cortical auditory processes [Dehais et al., 2016; Molloy et al., 2015; Scannella et al., 2013]. There are four known ipsilateral anatomical pathways between the IFG and the STG/MTG by which these attentionally modulated processes on early auditory processing may take place. These include the arcuate fasciculus, the superior longitudinal fasciculus, the uncinate fasciculus, and the extreme capsule fiber systems [Friederici, 2009]. Further research needs to be conducted to determine which of these pathways are involved.

Contrary to a previous investigation that found a signature for inattentional deafness only for late cortical auditory processes [Giraudet et al., 2015], we demonstrated that the inattentional deafness phenomenon might be driven by an attentional bottleneck that impairs the early processing of auditory stimuli. This result draws a clear distinction between inattentional deafness and inattentional amnesia [Kreitz et al., 2016; Wolfe, 1999], as the

◆ Neural Signature of Inattentional Deafness ◆

origin of alarm misperception is visible from perceptual stages. In addition, previous studies on change deafness [Downar et al., 2000, 2001; Puschmann et al., 2013] suggested that late stimuli processing is modulated by a network involving the Temporoparietal Junction (TPJ). Despite this evidence, our study showed no involvement of this region in alarm misses. This result is also in accordance with an attenuation of early cortical auditory processes rather than a failure to trigger late change-related cortical processes.

Interestingly, significant differential activity in visual motion processing area V5 for the audio misses > audio hits contrast (and the conjunction analysis), is consistent with the hypothesis that visual load plays a role in the generation of inattentional deafness. This is consistent with higher activation of the visual cortex observed by Molloy et al. [2015] during the high visual load conditions that elicited inattentional deafness. It should be noted however that these authors found visual modulation in other regions of the visual cortex, such as BA17 and 18. Such difference can be explained by the nature of their paradigm (visual search task in a static environment) and ours involving a dynamic visual environment.

It should be pointed out, however, that although the effective connectivity was reduced between the IFG and STG for audio misses relative to audio hits there was no significant difference in overall activity in the STS/MTG as determined by ROI analyses between the two conditions. This is contradictory with a recent study that suspected this associative auditory cortex to play a cross-modal gating role [Molloy et al., 2016]. However, these authors did not perform hit versus miss contrasts presumably because the miss rate was too low. These authors found the modulation of STS/MTG by comparing visual load levels. The results from some studies suggest that attentional modulation may facilitate auditory perception by a process of frequency-specific phase resetting without affecting the overall magnitude of the amplitude of the auditory response in these frequency ranges [Calderone et al., 2014; Ponjavic-Conte et al., 2012]. Furthermore, it has been proposed that entrainment (phase resetting) of neural oscillation may be a mechanism of selective attention [Calderone et al., 2014]. It is possible that suppression for audio misses relative to hits in STS/MTG was not found in our study because fMRI (having relatively poor temporal resolution) is not as sensitive to differences in phase but rather overall amplitude of neural activity.

The fMRI results associated with good performance (gates passed > gates missed) at the piloting task showed that regions of the dorsal striatum were associated with greater performance. This is in accordance with the involvement of this region in instrumental conditioning (stimulus-action-outcome association) and task performance [Atallah et al., 2007; O'Doherty, 2004]. This is also in line with an fMRI study [Adamson et al., 2014] that showed higher caudate nucleus (a part of the dorsal

striatum) activity was associated with flying accuracy. According to these authors, this activation underpins a better control of saccadic eye movements that ensure efficient cockpit scanning and better flying performance. On the contrary, the poor performance observed among participants together with the widespread activation associated with poor performance at this complex task provides a likely explanation for the absence of significant activations during video alarms misses: It is likely that their gaze only rarely moved toward the instrument panel, as the most dynamic part of the task was located at the top of the screen. In consequence, the large number of video alarm misses compared to audio alarm misses in our experiment could be attributed to the limited use of the instrument panel by the participants rather than to inattentional blindness. This is consistent with previous findings demonstrating that auditory alarms were more efficient [Wheale, 1981] than their visual counterparts as they provide information for pilots without requiring additional head/gaze movements [Edworthy et al., 1991] that could interfere with their visually driven operation of the aircraft [Dehais et al., 2012, 2014]. Because performance on the visual task may result from gaze direction and not attentional processes, while the video misses > video hits contrast controls for button press and the associated decision making processes leading to a motor command, it may not control for attentional processes specific to inattentional deafness from that of inattentional blindness.

Further investigation is necessary to identify if similar and/or different neural substrates are responsible for inattentional deafness and inattentional blindness. In this case, we recommend the use of eye tracking methods to monitor the gaze of the participants and to present video alarms using a heads up display in which the alarms would be in the same visual field as the view out the cockpit window.

The nature of our multitask paradigm was designed in a way to try to induce occurrence of inattentional deafness/blindness. Participants were instructed to focus on the continuous flying task without crashing and at the same time to identify occurrence of audio and video alarms by button press. Besides the explicit instructions to focus on the flying task, its continuous nature, over that of the discrete nature of the alarm detection tasks, also likely contributes to greater selective attention to the flying task. One would predict, however, that when focused attention may have shifted to some degree to the audio perception task that performance on the flying task might degrade. Consistent with this hypothesis, it is interesting to point out that greater activity in auditory processing regions bilaterally (Fig. 3 and Table III) is present for the gates missed over the gates passed condition suggesting perhaps that they are paying greater attention to auditory processing and not enough on flying the plane.

This is the first study to show the neural signature underlying inattentional deafness. Our approach differed

from previous studies investigating inattentional deafness in that it contrasted directly the misses and hits in the alarm perception task. Previous studies of this phenomenon [Giraudet et al., 2015; Molloy et al., 2015] focused on the contrast between experimental conditions exhibiting different levels of attentional load, without directly investigating the neural activity underlying misses relative to hits. We argue that such an approach would be sensitive to the causes of inattentional deafness, while ours provides a neural signature of the inattentional deafness events that could be used to detect them.

Nevertheless, it should be pointed out that the nature of the paradigm chosen for this experiment (alarms hits and misses) combined with the experimental time constraints associated with fMRI offered little control over the number of trials per condition. As a result, a large number of participants had to be excluded from the analysis due to excessively low number of trials for some conditions (hit or miss) not allowing for modeling by the GLM in the SPM analysis. However, it is arguable that the nature of the inattentional deafness phenomenon makes it difficult to elicit in a sustained manner [Giraudet et al., 2015]. Further investigation is needed to propose an experimental paradigm allowing control over the number of hits and misses observed, while maintaining ecological validity. It should be noted that potential differences arising from different numbers of audio misses and hits for each participant was controlled for by using miss rate as a covariate of non-interest in analyzing the contrast of audio misses > audio hits. The results, using audio miss rate as a covariate of noninterest (Fig. 2D), are nearly identical to those given in Figure 2A suggesting that the difference in the number of misses and hits did not confound the results.

In addition to the limitations given above, a control condition (flying straight) also had to be removed due to inappropriate application of the condition rules by the participants, which resulted in not being able to have a contrast to investigate the general effect of task difficulty and its interaction with inattentional deafness. It should be pointed out, however, that the behavioral results showing that a greater percent of gates were missed on the flying task for audio misses than for audio hits are consistent with the hypothesis that greater workload (visual load) on the flying task results in an attentional bottleneck causing inattentional deafness.

Although a large number of participants were dropped from the experiment and not using events from the flying straight task as an experimental contrast, the reasons and criteria for exclusion (given above) are unlikely to unduly bias our results by inadvertently selecting a subset of data.

In our study, the evidence of the involvement of the SMFC/pre-SMA and the IFG in the phenomenon of inattentional deafness in ecological conditions paves the way to the use of these regions as neural signatures of this phenomenon in real-world conditions. Taking this knowledge

into account in the design of Brain Computer Interfaces monitoring alarm perception [Callan et al., 2015, 2016], one could develop neuroadaptive automation that could attempt to reduce the workload or to present the alarms in a more salient way when the regions associated with the attentional bottleneck are active [Régis et al., 2014].

ACKNOWLEDGMENTS

We would like to thank Sayaka Tanaka and Chie Kawakami for her extensive assistance in conducting the experiment and Akiko Callan for her assistance in translating instructions from English to Japanese. We would also like to thank the MRI technicians at the Center for Information and Neural Networks for their assistance in running the experiments.

REFERENCES

- Adamson M, Taylor JL, Heraldez D, Khorasani A, Noda A, Hernandez B, Yesavage JA (2014): Higher landing accuracy in expert pilots is associated with lower activity in the caudate nucleus. *PLoS ONE* 9:e112607. doi:10.1371/journal.pone.0112607
- Atallah HE, Lopez-Paniagua D, Rudy JW, O'Reilly RC (2007): Separate neural substrates for skill learning and performance in the ventral and dorsal striatum. *Nat Neurosci* 10:126–131.
- Bliss JP (2003): Investigation of alarm-related accidents and incidents in aviation. *Int J Aviation Psychol* 13:249–268.
- Brand-D'Abrescia M, Lavie N (2008): Task coordination between and within sensory modalities: Effects on distraction. *Percept Psychophys* 70:508–515.
- Callan DE, Durantin G, Terzibas C (2015): Classification of single-trial auditory evens using dry-wireless EEG during real and motion simulated flight. *Front Syst Neurosci* 9:11.
- Callan DE, Gamez M, Cassel DB, Terzibas C, Callan A, Kawato M, Sato MA (2012): Dynamic visuomotor transformation involved with remote flying of a plane utilizes the 'Mirror Neuron' system. *PLoS ONE* 7:e33873.
- Callan D, Gateau T, Gonthier N, Dehaes F (2016): Neural signatures of inattentional deafness in airplane pilots recorded in real flight with dry-wireless EEG. 1st Neuroergonomics conference, Paris, October 6–7.
- Calderone DJ, Lakatos P, Butler PD, Castellanos FX (2014): Entrainment of neural oscillations as a modifiable substrate of attention. *Trends Cogn Sci* 18:300–309.
- Calvert GA, Thesen T (2004): Multisensory integration: Methodological approaches and emerging principles in the human brain. *J Physiol Paris* 98:191–205. 10.1016/j.jphysparis.2004.03.018
- Causse M, Imbert JP, Giraudet L, Jouffrais C, Tremblay S (2016): The role of cognitive and perceptual loads in inattentional deafness. *Front Hum Neurosci* 10:
- Cox RW (1996): AFNI: Software for analysis and visualization of functional magnetic resonance neuroimages. *Comput Biomed Res* 29:162–173.
- Craik KJ (1948): Theory of the human operator in control systems. *Br J Psychol Gen Sect* 38:142–148.
- Culham JC, Cavanagh P, Kanwisher NG (2001): Attention response functions: Characterizing brain areas using fMRI activation during parametric variations of attentional load. *Neuron* 32:737–745.

AQ2 AQ1

♦ Neural Signature of Inattentional Deafness ♦

- Cvach M (2012): Monitor alarm fatigue: An integrative review. *Biomed Instrum Technol* 46:268–277.
- Dalton P, Fraenkel N (2012): Gorillas we have missed: Sustained inattentional deafness for dynamic events. *Cognition* 124: 367–372.
- Dehais F, Causse M, Tremblay S (2011): Mitigation of conflicts with automation use of cognitive countermeasures. *Hum Factors J Hum Factors Ergonom Soc* 53:448–460.
- Dehais F, Causse M, Régis N, Menant E, Labedan P, Vachon F, Tremblay S (2012): Missing critical auditory alarms in aeronautics: Evidence for inattentional deafness? In: *Proceedings of the Human Factors and Ergonomics Society Annual Meeting* 56: 1639–1643. Sage Publications.
- Dehais F, Causse M, Vachon F, Régis N, Menant E, Tremblay S (2014): Failure to detect critical auditory alerts in the cockpit evidence for inattentional deafness. *Hum Factors J Hum Factors Ergonom Soc* 56:631–644.
- Dehais F, Tessier C, Christophe L, Reuzeau F (2010): The perseveration syndrome in the pilot's activity: Guidelines and cognitive countermeasures. In: *Human Error, Safety and Systems Development*. Springer. pp 68–80.
- Dehais F, Roy RN, Gateau T, Scannella S (2016): Auditory alarm misperception in the Cockpit: An EEG study of inattentional deafness. In *International Conference on Augmented Cognition*. Springer International Publishing. pp 177–187.
- Dux PE, Ivanoff J, Asplund CL, Marois R (2006): Isolation of a central bottleneck of information processing with time-resolved fMRI. *Neuron* 52:1109–1120.
- Downar J, Crawley AP, Mikulis DJ, Davis KD (2000): A multimodal cortical network for the detection of changes in the sensory environment. *Nat Neurosci* 3:277–283.
- Downar J, Crawley AP, Mikulis DJ, Davis KD (2001): The effect of task relevance on the cortical response to changes in visual and auditory stimuli: An event-related fMRI study. *NeuroImage* 14: 1256–1267.
- Edworthy J, Loxley S, Dennis I (1991): Improving auditory warning design: Relationship between warning sound parameters and perceived urgency. *Hum Factors* 33:205–231.
- Eickhoff SB, Stephan KE, Mohlberg H, Grefkes C, Fink GR, Amunts K, Zilles K (2005): A new SPM toolbox for combining probabilistic cytoarchitectonic maps and functional imaging data. *NeuroImage* 25:1325–1335.
- Eklund A, Nichols TE, Knutsson H (2016): Cluster failure: Why fMRI inferences for spatial extent have inflated false-positive rates. *Proc Natl Acad Sci* 113:7900–7905.
- Friederici A (2009): Pathways to language: Fiber tracts in the human brain. *Trends Cogn Sci* 13:175–181.
- Giraudet L, St-Louis ME, Scannella S, Causse M (2015): P300 event-related potential as an indicator of inattentional deafness?. *PLoS ONE* 10:e0118556.
- Hasanain B, Boyd AD, Edworthy J, Bolton ML (2017): A formal approach to discovering simultaneous additive masking between auditory medical alarms. *Appl Ergonom* 58:500–514.
- Keitel C, Maess B, Schröger E, Müller MM (2013): Early visual and auditory processing rely on modality-specific attentional resources. *NeuroImage* 70:240–249.
- Kreitz C, Furlley P, Simons DJ, Memmert D (2016): Does working memory capacity predict cross-modally induced failures of awareness? *Conscious Cogn* 39:18–27.
- Lavie N, Beck DM, Konstantinou N (2014): Blinded by the load: Attention, awareness and the role of perceptual load. *Philos Trans R Soc B* 369:20130205.
- Macdonald JS, Lavie N (2011): Visual perceptual load induces inattentional deafness. *Attent Percept Psychophys* 73: 1780–1789.
- Macaluso E, Driver J (2005): Multisensory spatial interactions: A window onto functional integration in the human brain. *Trends Neurosci* 28:264–271.
- Molloy K, Griffiths TD, Chait M, Lavie N (2015): Inattentional deafness: Visual load leads to time-specific suppression of auditory evoked responses. *J Neurosci* 35:16046–16054.
- Murphy G, Greene CM (2016): Perceptual load induces inattentional blindness in drivers. *Appl Cogn Psychol* 30: 479–483.
- O'Doherty J, Dayan P, Schultz J, Deichmann R, Friston K, Dolan RJ (2004): Dissociable roles of ventral and dorsal striatum in instrumental conditioning. *Science* 304:452–454.
- Ponjavic-Conte KD, Dowdall JR, Hambrook DA, Luczak A, Tata MS (2012): Neural correlates of auditory distraction revealed in theta-band EEG. *NeuroReport* 23:240–245.
- Puschmann S, Sandmann P, Ahrens J, Thorne J, Weerden R, Klump G, ... Thiel CM (2013): Electrophysiological correlates of auditory change detection and change deafness in complex auditory scenes. *NeuroImage* 75:155–164.
- Rauss KS, Pourtois G, Vuilleumier P, Schwartz S (2009): Attentional load modifies early activity in human primary visual cortex. *Hum Brain Mapp* 30:1723–1733.
- Raveh D, Lavie N (2015): Load-induced inattentional deafness. *Attent Percept Psychophys* 77:483–492.
- Régis N, Dehais F, Rachelson E, Thooris C, Pizziol S, Causse M, Tessier C (2014): Formal detection of attentional tunneling in human operator–Automation interactions. *IEEE Trans Hum Mach Syst* 44:326–336.
- Rinne T, Stecker GC, Kang X, Yund EW, Herron TJ, Woods DL (2007): Attention modulates sound processing in human auditory cortex but not the inferior colliculus. *NeuroReport* 18: 1311–1314.
- Rinne T, Balk MH, Koistinen S, Autti T, Alho K, Sams M (2008): Auditory selective attention modulates activation of human inferior colliculus. *J Neurophysiol* 100:3323–3327.
- Santangelo V, Olivetti Belardinelli M, Spence C (2007): The suppression of reflexive visual and auditory orienting when attention is otherwise engaged. *J Exp Psychol Hum Percept Perform* 33:137–148.
- Scannella S, Causse M, Chauveau N, Pastor J, Dehais F (2013): Effects of the audiovisual conflict on auditory early processes. *Int J Psychophysiol* 89:115–122.
- Scannella S, Roy R, Laour R, Dehais F (2016): Auditory neglect in the cockpit: using ERPIS to disentangle early from late processes in the inattentional deafness phenomenon. 1st Neuroergonomics conference, Paris, October 6–7.
- Scannella S, Pariente J, De Boissezon X, Castel-Lacanal E, Chauveau N, Causse M, Dehais F, Pastor J (2016): N270 sensitivity to conflict strength and working memory: A combined ERP and sLORETA study. *Behav Brain Res* 297:231–240.
- Sinnett S, Costa A, Soto-Faraco S (2006): Manipulating inattentional blindness within and across sensory modalities. *Quart J Exp Psychol* 59:1425–1442.
- Sörqvist P, Stenfelt S, Rönnberg J (2012): Working memory capacity and visual-verbal cognitive load modulate auditory-sensory gating in the brainstem: Toward a unified view of attention. *J Cogn Neurosci* 24:2147–2154.
- Szameitat A, Vanloo A, Muller H (2016): Central as well as peripheral attentional bottlenecks in dual-task performance

- activate lateral prefrontal cortices. *Front Hum Neurosci* 10:doi: 10.3389/fnhum.201600119.
- Tellinghuisen DJ, Cohen AJ, Cooper NJ (2016): Now hear this: Inattentional deafness depends on task relatedness. *Attent Percept Psychophys* 78:2527–2546.
- Tombu MN, Asplund CL, Dux PE, Godwin D, Martin JW, Marois R (2011): A unified attentional bottleneck in the human brain. *Proc Natl Acad Sci* 108:13426–13431.
- Vachon F, Tremblay S (2008): Modality-specific and amodal sources of interference in the attentional blink. *Percept Psychophys* 70:1000–1015. doi: 10.3758/pp.70.6.1000
- Wheale JL (1981): The speed of response to synthesized voice messages. *Br J Audiol* 15:205–212.
- Wickens CD (1984): Processing resources in attention. In: Parasuraman R, Davies DR, editors. *Varieties of Attention*. New York: Academic Press. pp 63–101.
- Wolfe JM (1999): Inattentional amnesia. *Fleet Memories* 17:1–21.
- Zäske R, Perlich MC, Schweinberger SR (2016): To hear or not to hear: Voice processing under visual load. *Attent Percept Psychophys* 78:1–8.
- Zeki S, Perry R, Bartels A (2003): The processing of kinetic contours in the brain. *Cereb Cortex* 13:189–202.

WILEY

Author Proof

AQ1: Please provide complete details for “Murphy et al., 2016; Causse, 2016; Awh et al., 2006; Molloy et al., 2016; MacDonald et al., 2011; Raveh et al., 2015; O’Doherty, 2004” in the reference list or delete the citations from the text.

AQ2: There is no mention of “Causse et al. 2016; Cvach 2012; Dalton & Fraenkel 2012; Dehais et al. 2011; Murphy & Greene 2016; O’Doherty et al. 2004; Raveh & Lavie 2015; Zäske et al. 2016” in the text. Please insert a citation in the text or delete the references as appropriate.

AQ3: Please confirm that given names (red) and surnames/family names (green) have been identified correctly.

Funding Info Query Form

Please confirm that the funding sponsor list below was correctly extracted from your article: that it includes all funders and that the text has been matched to the correct FundRef Registry organization names. If a name was not found in the FundRef registry, it may be not the canonical name form or it may be a program name rather than an organization name, or it may be an organization not yet included in FundRef Registry. If you know of another name form or a parent organization name for a “not found” item on this list below, please share that information.

FundRef name	FundRef Organization Name
Center for Information and Neural Networks	Center for Information Technology Center for Information Technology Research in the Interest of Society Hariduse Infotehnoloogia Sihtasutus Information Society and Media Directorate-General Information Technology Laboratory [NOT FOUND IN FUNDREF REGISTRY]
National Institute of Information and Communications Technology	Institute for Computing, Information and Cognitive Systems